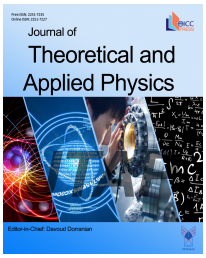

Volume 18, Issue 2, 182424 (1-13)

Journal of Theoretical and Applied Physics (JTAP)

https://dx.doi.org/10.57647/j.jtap.2024.1802.24

Effect of corona discharge modification on the surface properties of Polyacrylonitril/Thermoplastic polyurethane nanofiber membrane

Mohammad Mehdi Nikkhah Nikkho[1], Kambiz Tahvildari[1,*], Mohammad Allah Gholi Ghasri[2], Sima Habibi[3], Shirin Nourbakhsh[3]

[1]*Department of Chemistry, North Tehran Branch, Islamic Azad University, Tehran, Iran.*
[2]*Department of Chemistry, Yadegar-e-Imam Khomeini (RAH) Shahre Rey Branch, Islamic Azad University, Tehran, Iran.*
[3]*Department of Textile Engineering, Yadegar-e-Imam Khomeini (RAH) Shahre Rey Branch, Islamic Azad University, Tehran, Iran.*

[*]**Corresponding author:** k-tahvildari@iau-tub.ac.ir

Original Research

Received:
14 August 2023
Revised:
15 November 2023
Accepted:
13 January 2023
Published online:
10 March 2024

Abstract:

In this research, the effect of corona discharge surface modification on surface properties and water purification efficiency of electrospun polyacrylonitrile and thermoplastic polyurethane (PAN/TPU) nanofiber membranes has been investigated. The corona-treated PAN/TPU membranes were studied using field-emission scanning electron microscopy (FE-SEM), attenuated total reflectance–Fourier transform infrared spectroscopy (ATR–FTIR), water contact angle, detection and enumeration of *Escherichia coli* (*E. coli*), the most probable number (MPN) estimation of *E. coli*, and the desalinating performance through electrical conductivity (EC). The results showed that the sample PT4, which was subjected to 40 s of surface treatment, presented the lowest water contact angle (25.2°). The highly connected nanofibers between pores for the sample with 40 s surface treatment provided excellent membrane filterability. The formation of polar oxygen groups was confirmed on the surface of membranes contributing to its enhanced wettability. The desalination process provided good efficiency by removing about 30 wt.% of the salt present in the water samples. The MPN and lactose consumption tests indicated that the prepared membranes could remove *E. Coli*, however, fungi agents could pass it for both water samples of Persian Gulf and Caspian sea. The water hardness for the water samples of the Persian Gulf and Caspian sea were 6800 and 3700 ppm, respectively, indicating that both water samples are very hard. The appropriate purification of these samples sounds a way out to increase available drinkable and more pure water.

Keywords: Electrospinning; Nanofiber; Surface treatment; Water purification; Desalination

1. Introduction

Many communities are threatened by water shortage and its low quality. The need for safe water for agriculture, drinking, electricity and industry increases as the global population grows [1]. Bacteria and pathogens may also contaminate drinking water and cause death if it is acquired from surface water without treatment or is polluted due to the breakage of pipelines and long-time storage [2–4]. As a result, effective drinking water purification is hugely vital [5].

Despite dramatic reductions in energy demand over the last two decades, saltwater desalination methods are still very energy-demanding [6]. Electrochemical disinfection has been suggested as a possible alternative disinfection approach in recent years due to its low cost and effectiveness in killing a broad range of bacteria [7, 8]. The development of electrode materials with higher efficacy and a mix of ad-

sorption, conductive, and electro-oxidation capabilities has recently been emphasized. For electrochemical disinfecting, conductive nanosponge electrodes [9], flake graphite intercalation composite adsorbent [10], and Ti_nO_{2n-1} ceramic reactive electrochemical membrane electrodes [11] were constructed and tested. These devices display electrochemical disinfection integrated with adsorption and filtration [12]. Antibacterial nanofibres were also included in the composite membrane of electrochemical disinfection systems, allowing for bacterial entrapment and inactivation even when no electric field was present [13–16]. Therefore, nanofibre membranes with controlled porosity architectures have been successfully produced and utilized for water purification using electrospinning to improve the effectiveness of the purification process [17–21].

Thermoplastic polyurethane (TPU) and Polyacrylonitrile (PAN) are two materials that are used normally as membranes because of their outstanding physicochemical stabilities [22–24]. Acrylic (PAN) is a hydrophilic polyacrylonitrile copolymer and is used to make ultra-filtration membranes, hollow fibers for reverse osmosis, textile fibers, and oxidized PAN fibers [25]. TPU is a kind of polyurethane and is widely used due to its hardness, resistance to microorganisms and abrasion, and high hydrolytic stability [22, 26, 27]. This copolymer has a versatile use in producing hollow fibers for reverse osmosis, ultra-filtration membranes, oxidized PAN fibers, textiles, etc [28].

One of the ways of improving the efficiency of PAN/TPU filter membranes is modifying the surface of these membranes, which leads to an increment in the wettability of the surface and improves the adherence of glues, inks, and coatings to these polymer-based substrates. One of the widespread ways of surface treatment in extrusion, converting, and plastic film industries is corona treatment which has been used since the 1950s [29]. Bombarding the surface of a plastic substrate with high-speed electrons makes the surface molecule bonds to be broken [30].

To increase the energy and wetting of the surface and also adhesion properties of the main polyolefin such as Polypropylene (PP) and low-density polyethylene (LDPE), the use of oxidized functional groups have been recommended [31–35]. Different characteristics such as surface hardness [36], heat sealability [37], printability [38, 39], coatability [40, 41], and friction [42] are assessed to investigate the influence of corona treatment of polyolefins. The surface hydrophilicity of composites synthesized from graphene nanoplatelets and linear low-density polyethylene (LLDPE) was improved after corona treatment [43]. Making a functional group on the surface of Polypropylene film by corona discharge and its eminent role in connecting the polymer to the resin was studied by Ghorbani et al. [44]. The adhesion properties of LLDPE via corona treatment, investigated by Popelka et al., was improved [45]. Corona discharge was also used in the surface treatment of monofilaments of poly (ethylene terephthalate) (PET), polyamide-6 (PA-6), and polypropylene (PP). Based on the results, the surface morphology alteration and oxidation resulted from corona treatment effectively improved the wettability of polymeric surfaces but the bulk thermal properties were not affected [46]. The separation efficiency of an oil-in-water emulsion by membranes with a pore size of around 0.01 μm based on polysulfonamide with a molecular weight cut-off of 20 kDa treated by unipolar-corona discharge treatment, investigated by Alekseeva et al., intensified via the corona discharge treatment of the membrane surface [47]. Low temperature plasma techniques can be used for tailoring the surface properties of polymer membranes. The energized species in the plasma include ions, electrons, radicals, metastables, and photons. An appropriate selection of the plasma source and operating parameters allows introducing various functional groups onto membrane surfaces [48]. Therefore, corona discharge modification could significantly enhance PAN/TPU nanofiber membrane properties for water purification applications; however, there were limited studies regarding applying corona discharge to modify PAN/TPU nanofibre membranes for water treating purposes. Given that, the electrospinning method was used to fabricate the nanofibre membranes of PAN/TPU with enhanced mechanical properties, controllable porous structures, and uniform diameters. The effects of this modification on the properties of the PAN/TPU membrane were evaluated using FE-SEM, ATR–FTIR, and water contact angle evaluation. Its water purification efficiency was examined through microbial tests, including disinfection performance, detection, and enumeration of *Escherichia coli* (*E. coli*), as well as the most probable number (MPN) estimation of *E. coli*. In addition, the desalinating performance of the membrane was measured through electrical conductivity (EC) and complexometric titration measurements.

2. Materials and methods

2.1 Preparation of PAN/TPU electrospun nanofibres

0.5 g of PAN and 0.5 g of TPU were separately dissolved in 5 mL of Dimethylformamide (DMF), respectively at 25° C in a paraffin-covered beaker and were stirred for 24 h using heater stirrer to prepare initial electrospun solutions. The ratio of 30% PAN and 70% TPU was used for blending PAN/TPU. The homogeneous electrospun solution of PAN/TPU (10 wt%) was formed after adding 3.5 cc TPU solution to 1.5 cc PAN solution and mixing with a heater stirrer at room temperature for 24 h. A nanofiber electrospinning unit (Kato Tech Co. LTD, Japan) was used to implement the electrospinning process. The carriage included 5 cc of the polymer solution and an active electrode parallel to the collecting electrode. A voltage of 15 kV and a feeding rate of 0.04 mm/min were applied to deliver the 180 mm of the spinning solution from the active electrode to the collecting electrode via moving carriage at the temperature and relative humidity of $\sim 25°$ C and $35-45\%$, respectively. The distance between the nozzle and the collector was 15 cm. Two layers of aluminum foil were used for collecting fabric. To remove the residual solvent, the PAN/TPU electrospun nanofibers were dried in a vacuum oven.

2.2 Corona treatment

A commercial device Saba Electric, Iran with AC frequency between $10-50$ kHz was used for the corona treatment of fabrics at atmospheric pressure. Different membranes were

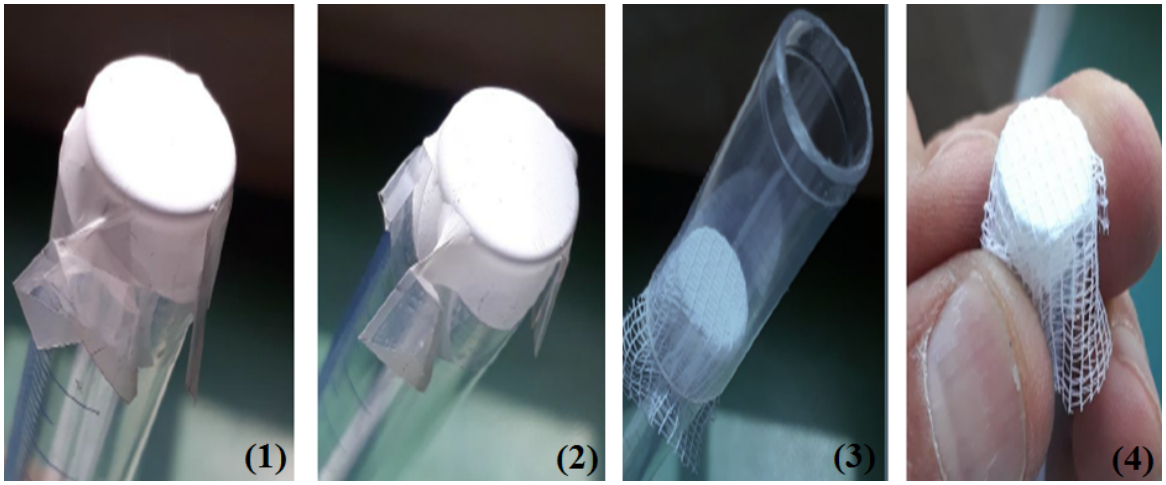

Figure 1. Image of the preparing process of PAN/TPU membrane (PT4) for disinfection performance test.

placed on separate silicone drums to be subjected to various rounds of surface treatment with the amperage of 2.45 A, the voltage of 539 V, and the treatment time of 10 s for each surface treatment round. Therefore, different membrane samples were exposed to plasma for 20, 30, 40, 50 and 60 seconds. The treatment was done for several times because of achieving total treatment time. The coding of samples according to each surface treatment round applied to them are presented in Table 1.

2.3 ATR–FTIR analysis

According to dual functionality of FTIR device and the composite material's solidity, ATR capability is utilized for solid samples and FTIR capability is used for liquid samples. The characteristic peaks recorded by ATR–FTIR (TENSOR 27, BRUKER Co.) were used to confirm the presence of PAN and TPU polymers. The FTIR test was conducted on the PAN/TPU composite solution (liquid sample) while the ATR test was perfomed on the electrospinned nanofibers (solid sample). The samples were put directly on the sample holders. The recorded spectra were in the range of 400 – 4000 cm^{-1}, with a spectral resolution of 4 cm^{-1} and an average rate of 32 scans min^{-1}.

2.4 Microstructural analysis

Using the ZEISS Ultra-Plus device, FE-SEM micrographs of the surface morphologies of sieved bacteria and the membranes were obtained. To avoid charging, a fine coater of JEOL JFC-1200 was employed to apply a layer of Au–Pd alloy on the surface of the samples. A UTHSCSA Image Tool 3.0 image processing software was used to determine the average diameter.

Table 1. Coding of membrane samples according to each surface treatment round.

Sample Code	Rounds of surface treatment	Treatment time (s)
PT2	2	20
PT3	3	30
PT4	4	40
PT5	5	50
PT6	6	60

2.5 Eelectrical coductivity

The electrical conductivity of several dilutions of NaCl solution (5, 10, 15, 20, 500, 1000, 2000 ppm) was determined by an EC meter using the EC potentiometric technique (inolab cord 730, Laboratory Conductivity meter). The conductivity was measured before and after applying the PAN/TPU filter membrane (PT4) to each NaCl solution, and the EC meter was calibrated with KCl.

2.6 Water contact angle

For measuring the contact angles in DSA-20E (Kruss, GMBH, Germany), water droplets (2 μL) were dropped on the fibrous mat surface freely. Five different measurements were taken at a different portion of the mat surface and for each mat, the average results were considered [49].

2.7 Detection and enumeration of *E. Coli*

An image of the PT4 prepared PAN/TPU membrane during the filtration tests is shown in Fig. 1. The initial disinfectant column had the diameter of 1.5 cm, and the prepared membranes had the surface area of 2.5 cm^2.
Eosin methylene blue (EMB) and sorbitol MacConkey (sMac) agar (Difco) plates were inoculated with 0.1 mL of water samples and incubated overnight at 37° C to identify *E. coli*. The counts were then expressed as CFU/mL of the sample at the highest dilutions using sterile saline. Non-sorbitol fermenting colonies were subcultured on blood agar plates, incubated overnight at 37° C, and then tested using *E. coli* O157 antiserum in a slide agglutination test (Difco). Other *E. coli* serotypes were not tested in this investigation [50].

2.8 MPN estimation for *E. coli*

Cultures were initially diluted to an optical density of 0.2600 nm ($\sim$ 8.0 $\log_{10}$ CFU/mL), in phosphate-buffered saline (PBS), then to a predetermined density (see below) followed by 10-fold serially diluted in PBS, with vigorous

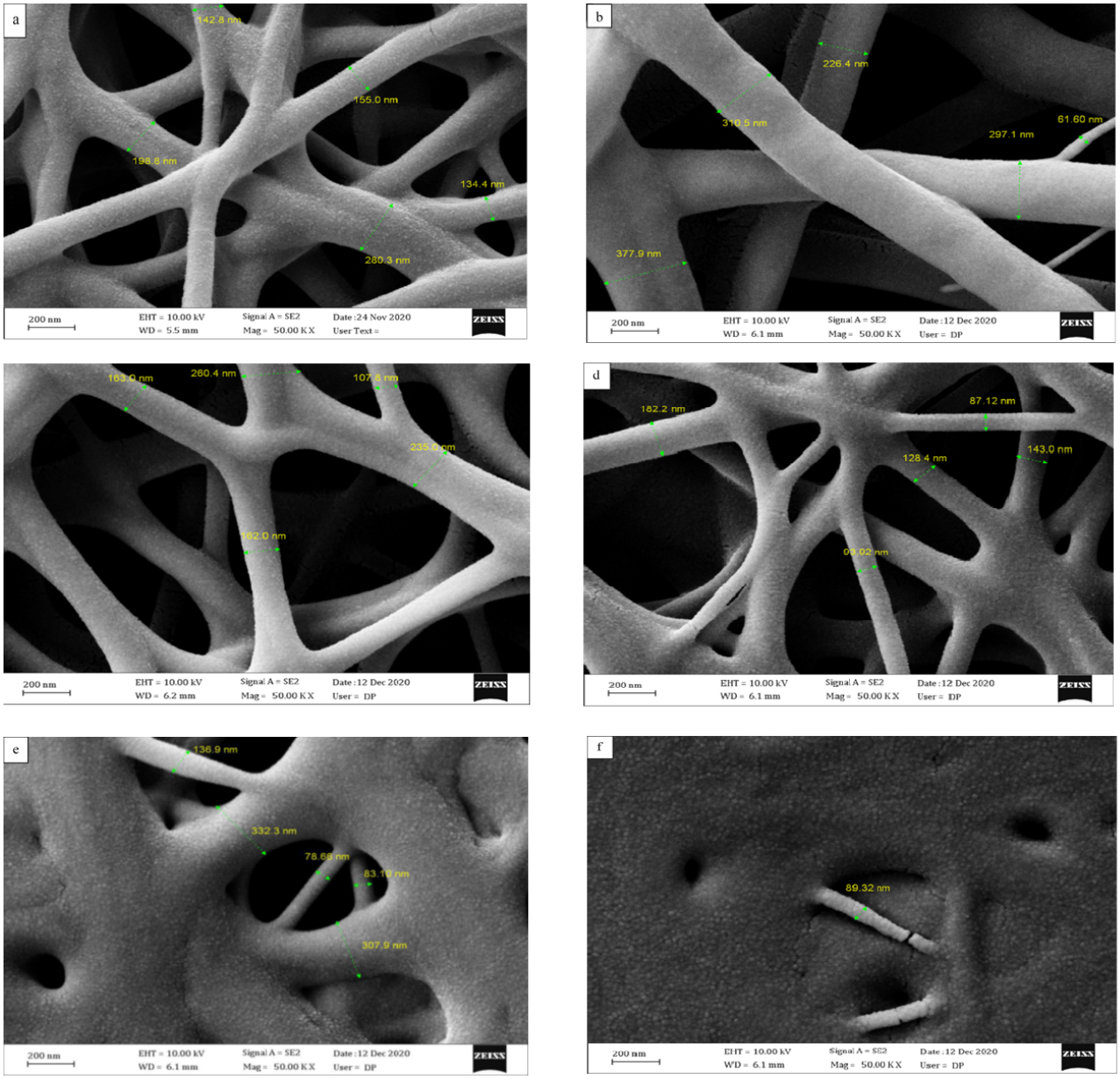

Figure 2. FESEM images of the surface morphology and the diameter of nanofibers after the electrospinning process for PT sample (a) and after surface treatment for PT2 (b), PT3 (c), PT4 (d), PT5 (e), and PT6 (f) samples.

vortex mixing between each step as the starting point for MPN estimation. Each bacterial dilution was collected in three duplicates of 100 μL each and cultured for 48 hours at 27° C in MacConkey broth purple (Oxoid/ThermoScientific; CM0505). The color shift from purple to yellow was used to measure growth. To ensure that no further color change occurred, the samples were incubated for another 24 hours. Finally, each stock solution was spread on MAC in 100 μL samples, incubated, and the quantity of dark red colonies was counted [51].

3. Results and discussion

3.1 FE-SEM

The surface morphology and the diameter of nanofibers after electrospinning and surface treatment obtained from FE-SEM images are presented in Fig. 2. As has been shown in Fig. 2, the surface modification process triggers the melting of nanofibers into each other, and for samples PT5 and PT6, the membrane degrades significantly. The surface morphology of samples PT, PT2, PT3, and PT4 is quite the same and nanofibers are roughly similar in diameter size, whereas by modifying the surface of the membrane in samples PT5 and PT6, an interconnected structure, resulted from the melting of nanofibers, was observed. The average diameter of the nanofibres was about 200 nm. Moreover, the electrospun nanofibres were uniform and highly connected between pores for the samples PT, PT2, PT3, and PT4, which provides excellent membrane filterability. To determine the best permeability and wettability of these membranes, the test of water contact angle has been carried out. However The FESEM images show that the PT4 membrane, which has undergone four rounds of treatment, has the most ideal structure due to its highest porosity and

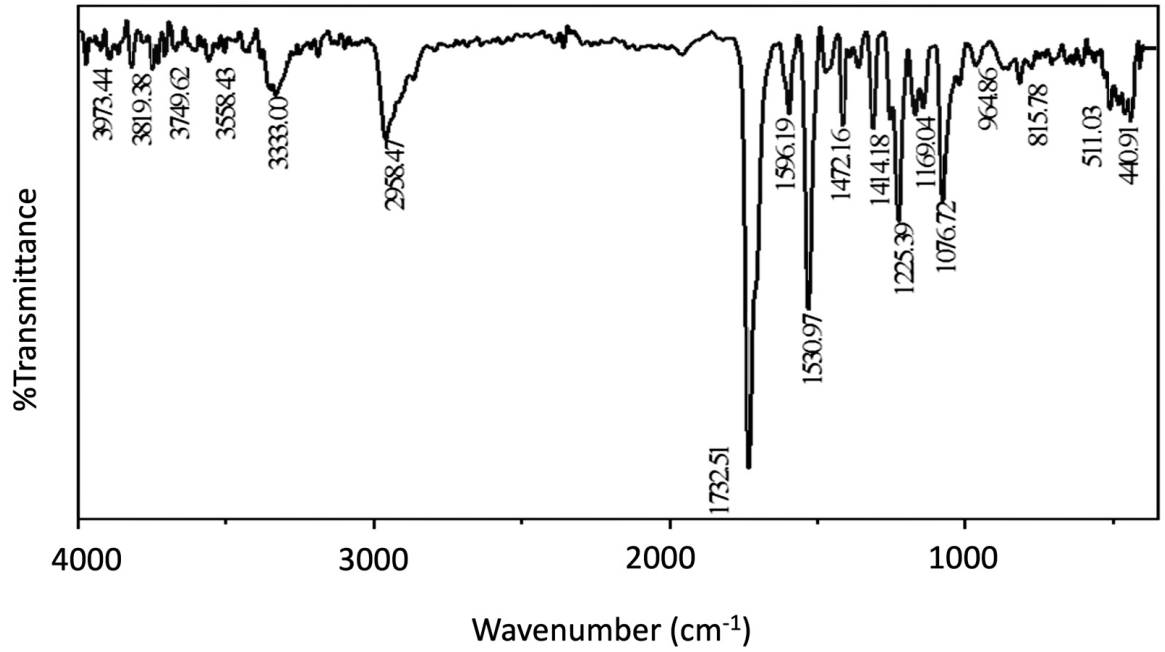

Figure 3. FTIR spectra of the PAN/TPU liquid composite without plasma surface modification.

lowest fiber diameter of seven. As a result, the highest penetrability is anticipated. PT4 has smaller internal nanofiber connection diameters than any other sample. Furthermore, more internal nanofiber connections maximize the surface area that passing water comes into contact with, leading to optimal filtration performance. On this basis, PT4 membrane was chosen as the main membrane in the experiments.

3.2 ATR–FTIR analysis

The corona treatment can change the chemical composition of the surface of PAN/TPU samples. The FTIR spectra of untreated PAN/TPU liquid composite have been shown in Fig. 3. The transmittance peaks of Fig. 3 present peaks attributed to PAN located at 1674.24 cm^{-1} correspondings to C=O bond, 659.94 cm^{-1} correspondings to C-H bond, as well as 1095.13 cm^{-1} and 1256.07 cm^{-1} correspondings to C-O bond. The band at 1388.36 cm^{-1} is consistent with C-H aliphatic group, and the one at 1439.56 cm^{-1} corresponds to C-H tensile vibration. The peaks located at 1674.24 cm^{-1} correspond to the C=C group, 2930.05 cm^{-1} correspondings to the C-H stretch, and 3516.68 cm^{-1} correspondings to the O-H group are also recognizable [52, 53]. Typical peaks of the electrospun TPU located at the wavelengths of 3334 cm^{-1} and 2969 cm^{-1}, observed on the shoulder of peaks situated in this range of wavelengths, identify the N-H stretching and the C-H stretching, respectively. The C=O stretching at 1726 and 1702 cm^{-1}, as well as N-H

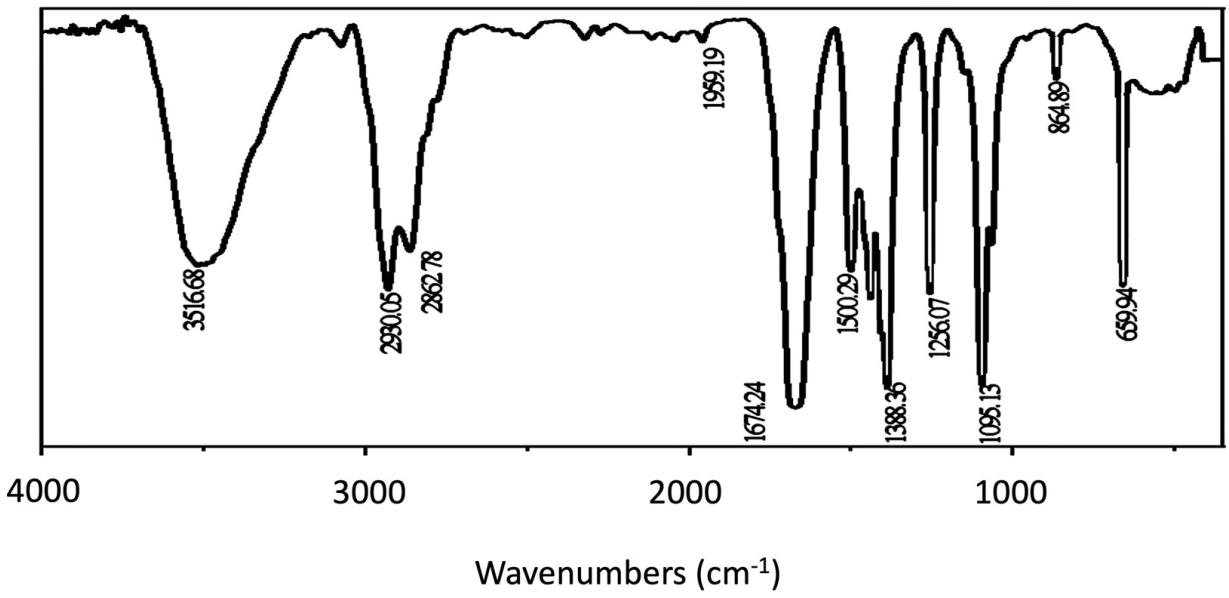

Figure 4. ATR spectra of the PT4 sample.

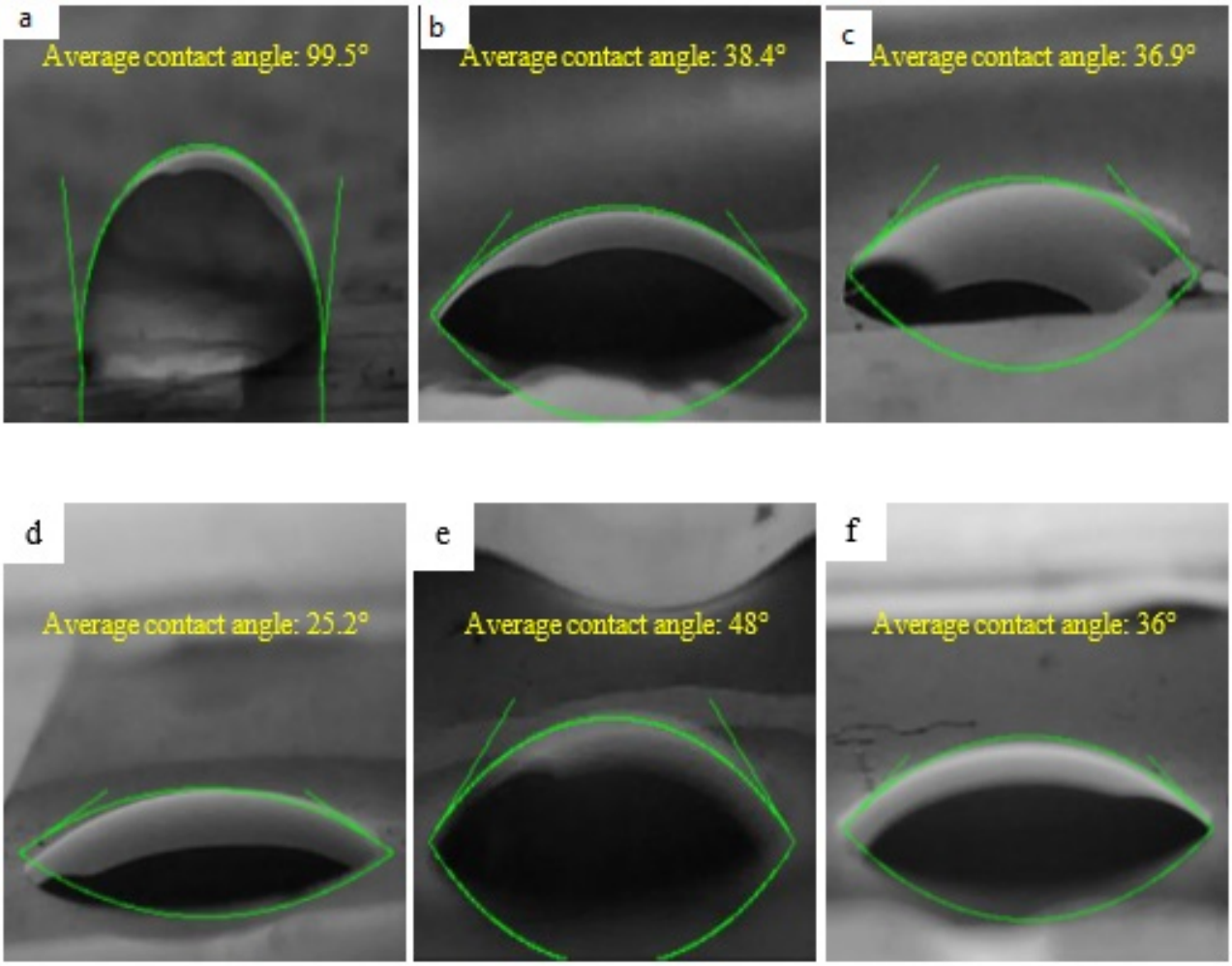

Figure 5. The contact angles of PT (a) PT2 (b), PT3 (c), PT4 (d), PT5 (e), and PT6 (f) membranes.

bending at 1595 cm^{-1}, are also placed at the shoulder of the large peak extended from about 1550 to 1750 cm^{-1}. C-C stretching at 1418 cm^{-1} as well as C–O–C stretching at 1169 and 1078 cm^{-1} are also observable [54, 55]. Additionally, the range of 3200 to 3500 cm^{-1}, attributed to the O-H stretch, confirms the presence of the hydroxyl group formed due to the presence of environmental humidity during the surface modification with corona [56]. Additionally, PAN and TPU spectra are given separately before blending in Fig. 10 [57, 58].

In order to confirm the effect of plasma on the surface of membranes and comparing the changes of all samples obtained from the membrane modification, the ATR-FTIR test has been used. Fig. 4 shown ATR spectra of the solid PAN/TPU composite with plasma surface modification (sample PT4) changing polarity. The ATR-FTIR results of Fig. 4 present bands associated with symmetric and asymmetric vibrations of $–CH_2–$ (2956 cm^{-1}), asymmetric C–H (1458 cm^{-1}), and symmetric C–H (1358 cm^{-1}) bending in-plane. Corona treatment on PAN/TPU changed the spectrum by increasing the transmittance intensity of peaks as well as incorporating a variety of functional oxygen groups, which will probably change the wettability. New transmittance bands also appeared, like those linked with vibrations of C=O or C=O in the carboxyl group located in the region of $1800 - 1500$ cm^{-1} and C–O vibration at 1200 cm^{-1} as well as a wide band associated with the vibration of –OH in the region of $3200 - 3500$ cm^{-1}. These new bands illustrated the polar oxygen group, which probably plays a major role in the increase of samples' wettability. As showed in Fig. bx ,the differences between ATR spectra results have presented that the binding of polar groups to the treated membrane increases, which provides efficiency to the membranes against the ions present in the water. Due to the performance of these membranes in the normal environment, the humidity of the atmosphere in the plasma environment causes the formation and replacement of hydroxyl groups in the membrane structure, which is noticeable in the range of 3300 cm^{-1}; however, there is no hydroxyl group present in the structure of PAN/TPU that indicates the effect of plasma on membranes.

3.3 Water contact angle test

Chemical composition has a major influence on the surface hydroscopic and wettability behavior of membranes. While non-polar bonds provide low wettability, polar bonds are responsible for the hydrophilicity of surfaces. Wettability of the membrane, the ability of a liquid to maintain contact with a surface, was determined using water contact angle

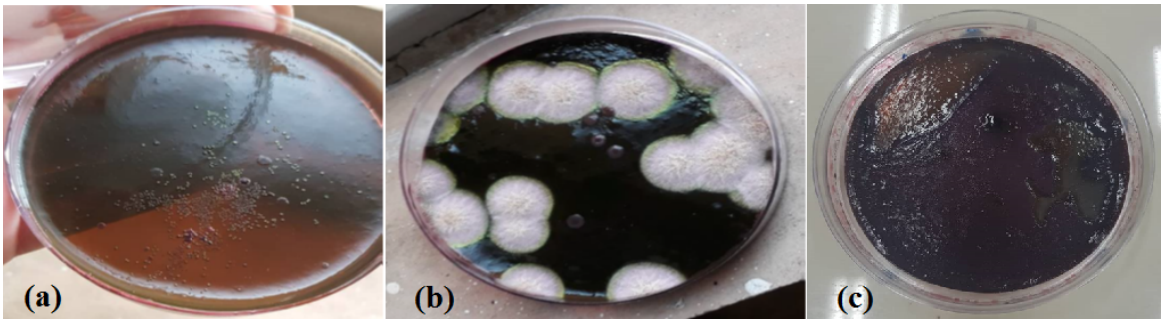

Figure 6. The results of culturing *E. coli* before (a) and after (b) the addition of the Persian Gulf water sample, indicating the presence of fungus and *Escherichia coli*. (c) *E. coli* culture result on EMB medium after Persian Gulf water passes through the designed membrane.

tests. Fig. 5 presents the contact angles of six different membranes subjected to surface modification as well as the one without any surface modification. As has been presented in Fig. 5(a), the untreated surface of the PAN/TPU illustrates strong hydrophobicity with a contact angle of 99.5°. The contact angles of all the other modified surfaces presented significant reduction by achieving relatively low values ranging between 25.2° to 48°, indicating high wettability and hydrophilic nature. Corona discharge plasma treatment of PAN/TPU increased its wettability by functionalizing its surface.

The highest wettability was observed in the PT4, while the lowest one was attributed to the PT5 sample, which exhibited melted nanofibers microstructure in its FE-SEM images. The occurrence of the increased wettability of the surface-treated membrane is likely to be associated with the surface oxidation and formation of free radicals and polar functional groups on the surface of membranes after corona treatment. Moreover, the variations in the surface morphology could also play a role in this behavior of the material. The surface area and pore content of the PT4 sample is high, according to Fig. 2(d), which increases the amount of functional groups that can react with water drop. The increase of the contact angle value for the surface of the PT5 sample (Fig. 5(e)) as compared to other treated ones could be attributed to the change of surface morphology and the melting of nanofibers, which highly decreases the surface area and pore content of this membrane as well as decreasing the amount of functional groups capable of reacting with water drop, as confirmed by the FE-SEM images. ATR analysis comparing the intensity of transmittance peaks assigned to hydroxyl groups (Fig. 8) has also confirmed that the membrane PT5 (the less hydrophilic membrane among other surface-treated ones) has lower amount of functional groups, obviously due to its decreased surface area (Fig. 2(e)). However, applying further surface treatment rounds (on sample PT6), despite the increased proportion of melted nanofibers and decreased pore content or surface area, has caused improved wettability of the membrane in comparison to that of the PT5. This can be attributed to the degradation of the polymers and increased amount of functional groups per unit area caused by the longer treatment time of this membrane, which has partly limited the adverse effect of the reduced surface area.

Figure 7. Images of tubes before (up) and after (down) subjection to the MPN test.

3.4 Desalination performance and electrical conductivity

Desalination methods have gained much interest during the last decades as a convenient way for providing potable water. This process includes the elimination of soluble salt in the water to achieve less than 1000 mg/L of salts or total dissolved solids (TDS). Above the mentioned level of salt, water properties including odor, corrosion propensity, color, and taste significantly affect its quality. The WHO and the Gulf Drinking Water Standards suggest a standard of 1000 mg/L TDS for drinking water [59]. In reverse osmosis of the membrane, the pressure pushes water into the membrane to dismiss a large number of its ions resulting in the obtainment

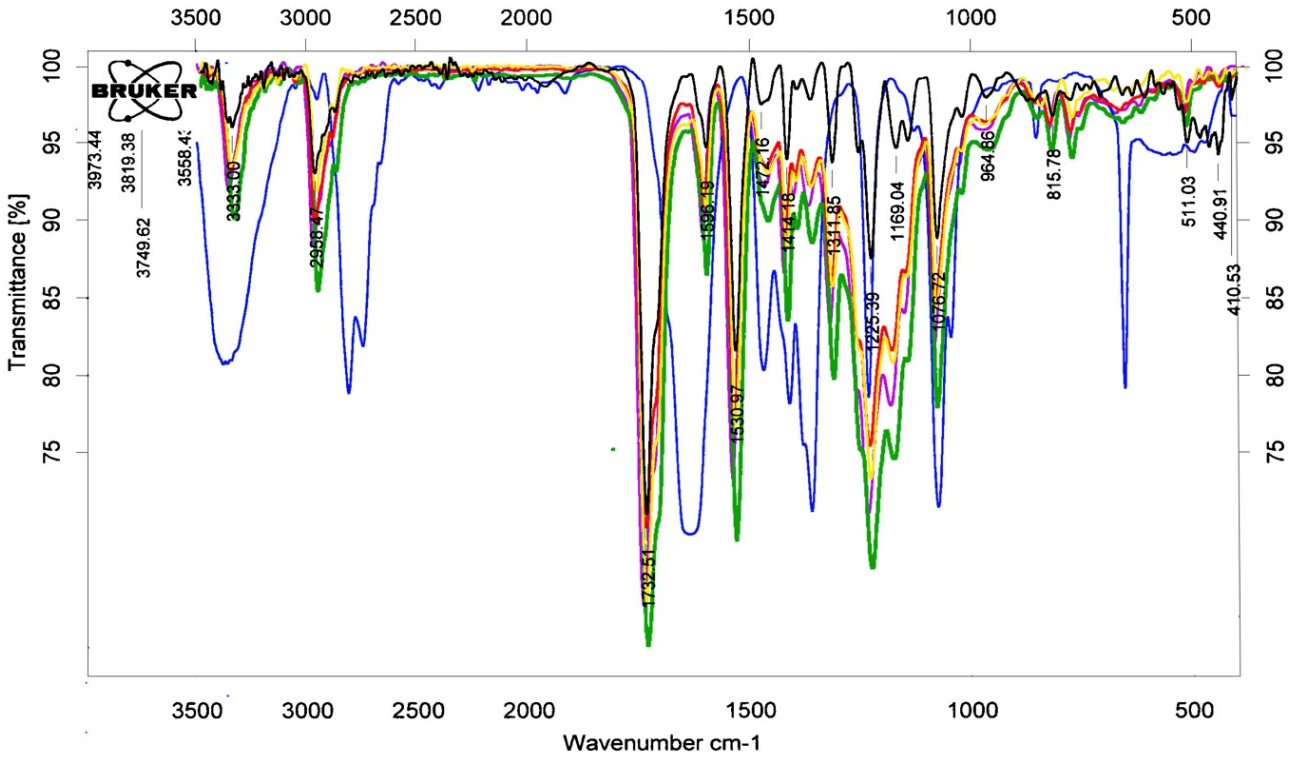

Figure 8. Comparison between different stages of treatment. (black) primary membrane with no treatment. (red) 20s treating. (green) 30s treating. (blue) 40s treating with best absorbtion. (yellow) 50s treating. (purple) 60s treating.

of water with limited mineral content. Conductivity is a beneficial method carried out in desalination tests to measure the performance of membranes in the reverse osmosis cycle, as the minerals in seawater are normally ionic [60, 61]. As the FE-SEM images, water contact angle results and ATR-FTIR analysis showed that the PT4 membrane had the most appropriate structure for water penetration, now and here we shoud test its purification activity on salty water. The efficiency of identical PT4 membranes determined by the results of electrical conductivity for various NaCl solutions with the concentrations of 5, 10, 15, 20, 500, 1000, and 2000 ppm are presented in Table 2. Like other methods for purifying salty water, to reach the standard of potable waters, the number of desalination process rounds increases.

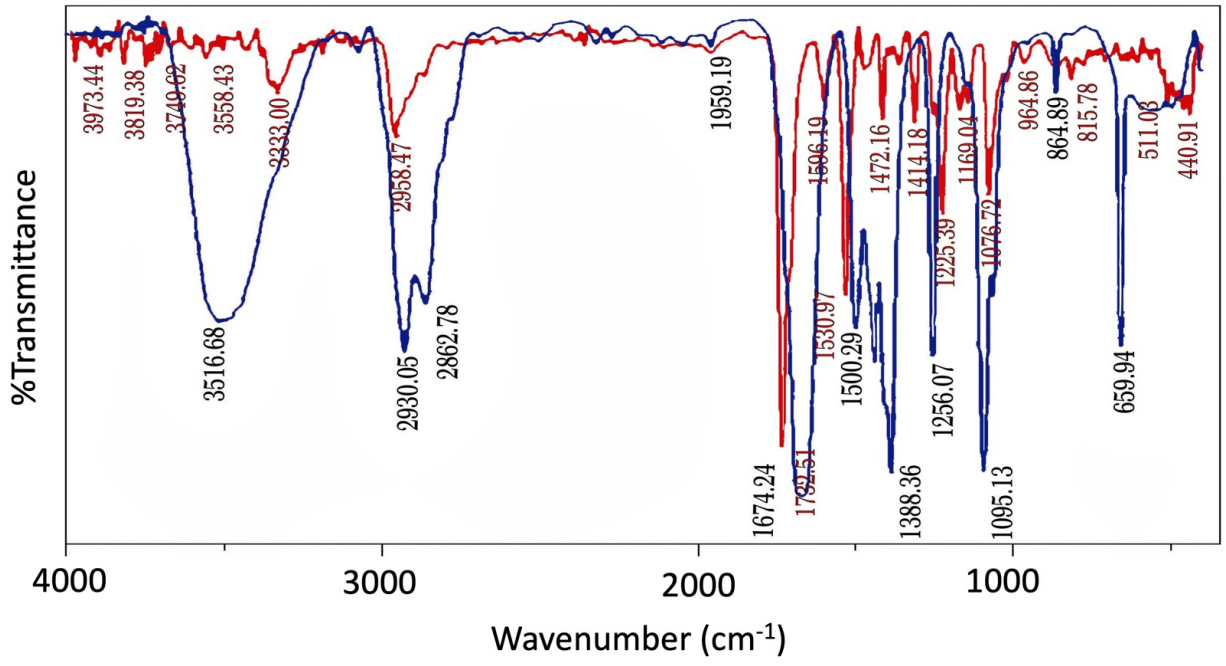

Figure 9. ATR spectra of treated (blue) and untreated membrabe (red)

Regarding the Caspian Sea and the Persian Gulf water, the result presented in Table 2 is achieved after six rounds of the desalination process. After applying the desalination process, the TDS amounts of the prepared solutions reach below the WHO and the Gulf Drinking Water Standards (1000 mg/L). The desalination process adopted with the help of surface-treated electrospun PAN/TPU membrane for the water samples with various concentrations as well as those of the Caspian and Persian Gulf Seas presents good efficiency by removing about 30 wt.% of the salt presented in the water samples. According to percentage of desalination in Table 2 the amount of desalination in 1000 to 2000 ppm decreases because of monolayer filteration. If there are multiple filteration layers, the amount of purification will also increase. The effect of purifying Nacl solution at 1000 ppm on PT4 membrane is 72% and a significant amount. However, the TDS values of the Caspian Sea and Persian Gulf water samples do not reach below 1000 g/L even after six rounds of the desalination process. Cai et al. [62] studied membrane desalination through surface fluorination treated electrospun PAN membrane. The desalination performance of PAN membrane with nonwoven structure presented the salt rejection rate of $\geq 99.9\%$. In another study performed by Li et al. [63], the desalination performance of polyamide/Kevlar aramid nanofiber membrane was studied. The membrane showed an excellent water-salt separation performance, with a high rejection for NaCl salt (80.3%), tested in cross-flow filtration with 1000 mg L^{-1} salt solution at 6 bar, 25° C. Kaur et al. [64] also investigated electrospun PAN-based membrane composite and its impact on separation performance on thin-film composite nanofiltration membrane. The membrane was capable of rejecting 86.5% $MgSO_4$ at a permeate flux of 102 L/m^2 h at 70 psig. In another study performed by Tijing et al. [65], they prepared dual-layer (poly(vinylidene fluoride-co-hexafluoropropylene) and PAN) nanofibrous composite membrane by electrospinning and tested it for desalination performance. The nanofibrous membranes tested with 35 mg L^{-1} NaCl feed presented a salt rejection of $\geq 98.5\%$. Assiry et al. [59] have studied desalination process of seawater by investigating the effects of TDS, electrical field strength and temperature on electrical conductivity during ohmic heating. The range of conductivity during ohmic heating was $55 - 399.6$ (mS/cm) for TDS ranging between 37 and 130 PPT, which was strongly dependent on TDS and temperature. In another study, Talaeipoor et al. [66] investigated the NF90 and TW30 membranes nanofiltration (NF) and reverse osmosis (RO) by measuring total dissolved solids and electric conductivity. The percent of the salinity rejection was 50.21%, 72.82 and 78.56% in NF, RO and hybrid processes, respectively.

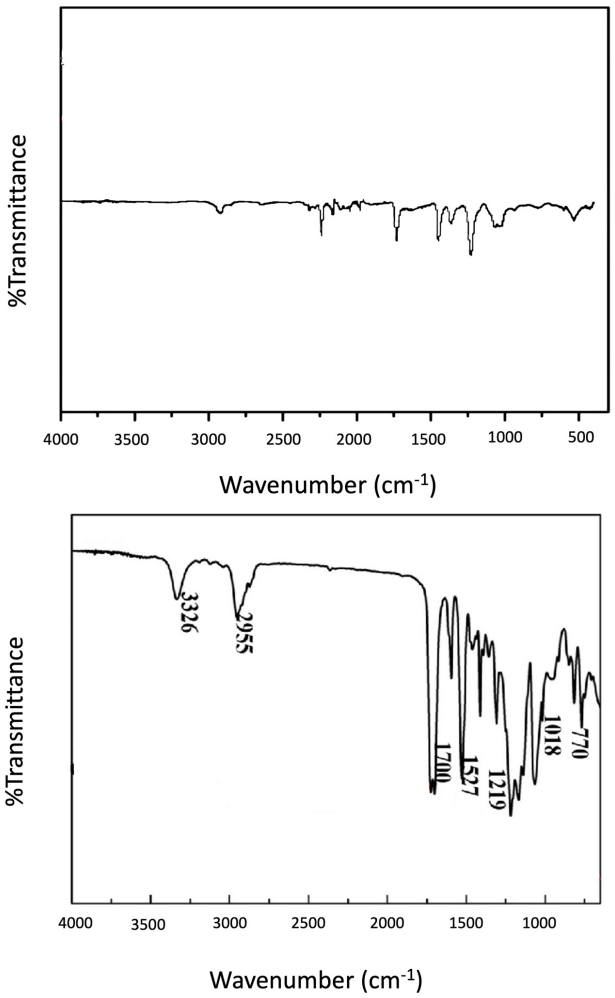

Figure 10. PAN (up) and TPU (down) FTIR spectra.

Table 2. Desalination performance of the surface-treated electrospun PAN/TPU membrane obtained through electrical conductivity test.

Sample (ppm)	TDS (mg/L) Before Desalination	EC (10^{-6} S/cm)	Sal	TDS (mg/L) After Desalination	EC (10^{-6} S/cm)	Sal	Percentage of desalination
5	19	19.1	0.0	3.2	3.24	0.0	-
10	25	25.1	0.0	4.23	4.25	0.0	-
15	36	35.6	0.0	6	6.1	0.0	-
20	45	45	0.0	7.61	7.63	0.0	-
500	1016	1011	0.3	172	171.5	0.0	-
1000	1961	1972	0.8	331.9	334.5	0.58	72.5
2000	-	3970	2	∼673	673.4	1.17	58.5
Persian Gulf	-	61400	41.3	∼1041	1041.5	28.6	69.24
Caspian sea	-	33400	22.47	∼5665	5665.8	15.7	69.87
Distilled water	7	7.2	0.0	-	-	-	

3.5 Detection and enumeration of *E. Coli*

Two droplets of the water of both the Persian Gulf Sea and the Caspian Sea were used in the culture medium of EMB. The *Escherichia coli* presented in this culture could consume the lactose and form red colonies with a metallic luster. This bacteria was identified in the samples from both the Caspian and Persian Gulf Sea, which is a sign of the presence of human and animal feces due to the entry of human sewage into the sea. Moreover, the water was infected with the fungus. Fig. 6 presents the results of culturing *E. coli* before (a) and after (b) the addition of the Persian Gulf water sample, indicating the presence of fungus and *Escherichia coli*. These results were the same for Caspian Sea water samples. The Water Sample from the Caspian Sea and the Persian Gulf was passed through the PT4 membrane and tested again on the EMB culture medium to ensure the biological purity of the membrane. Fig. 7 demonstrates the ability to disinfect the designed the membrane in the absence of *E. coli* in the EMB culture medium.

3.6 MPN estimation for *E. coli*

In order to determine the contamination level of the water samples on PT4, the most probable number (MPN) test was used. The change of culture's color to yellow due to its acidity and accumulation of SO_2 gas indicates the consumption of lactose present in the growing culture by *E. Coli*. Comparing the obtained results with the standard table of MPN, the number of *E. Coli* in 100 mL of water was estimated. The test results indicated that the color change and gas formation occurred in all the first three test tubes (choosing number 3 for this group). Regarding the second three test tubes, two of them presented color change and gas formation (choosing the number 2 for this group), and for the last group, one test tube responded positively to the test (choosing number 1 for the last group). Comparing test results with the standard table of MPN, led to the number of 17 (17 *E. Coli* were presented in 100 mL of water), indicating that both samples of water were highly infected with human and animal feces due to the entry of human sewage into the sea (grade 4). The results of the disinfection test indicated that the prepared nanofiber membranes operated efficiently in eliminating *E. Coli* from the infected water samples; however, their performance for removing fungus was not efficient. Fig. 8 shows the images of the test tubes before and after the MPN test, illustrating their color change.

3.7 Water hardness

The results of water hardness for the water samples of the Persian Gulf was 6800 ppm; while this value was 3700 ppm for the Caspian sea, indicating that both water samples are very hard as they exceed the level of 150 ppm, a maximum limit recommended for classifying water hardness.

4. Conclusion

In this research, the water purification performance of the surface-treated electrospun PAN/TPU nanofiber membrane has been examined. The surface of nanofiber membranes was treated by corona discharge plasma for enhancing the surface properties and porous structures of the membrane. Corona treatment of PAN/TPU composites played an important role in altering the surface and its wettability behavior. The most effective improvement in wettability was observed for PT4, which was resulted from functionalization processes, the introduction of oxygen-based polar groups, and surface morphology in the corona-treated surface confirmed by ATR-FTIR and FE-SEM results. The obtained results confirm that corona discharge plasma treatment provides a reduction in the water contact angle and leads to enhanced wettability of the membranes. Microbial tests such as disinfection performance, detection, and enumeration of *Escherichia coli*, most probable number (MPN) estimation of *E. coli* as well as desalination performance test through electrical conductivity (EC), and complexometric titration were employed to analyze the water purification efficiency of the corona-treated electrospun PAN/TPU membrane. The detection and enumeration tests of *E. Coli* confirmed the infection of the Persian Gulf Sea and Caspian Sea sample water with the *E. Coli* and fungus. MPN test has also given the number of 17 for the samples, presenting that water samples from both seas were highly infected. The results of the membrane efficiency for desalination of several water samples presented that the surface-treated electrospun PAN/TPU membrane provides good efficiency by removing about 30 wt.% of the salt contained in the water samples. The results of the disinfection test illustrated that the prepared nanofiber membranes operated efficiently in eliminating *E. Coli* from the infected water samples; however, their performance for removing fungus was not efficient.

Ethical approval
This manuscript does not report on or involve the use of any animal or human data or tissue. So the ethical approval is not applicable.

Authors Contributions
All the authors have participated sufficiently in the intellectual content, conception and design of this work or the analysis and interpretation of the data (when applicable), as well as the writing of the manuscript.

Availability of data and materials
Data presented in the manuscript are available via request.

Conflict of Interests
The author declare that they have no known competing financial interests or personal relationships that could have appeared to influence the work reported in this paper.

Open Access

References

[1] A. K. Biswas and C. Tortajada. *"Assessing global water megatrends, Assessing global water megatrends."*, volume . Springer, 2018.

[2] F. Edition. "Guidelines for drinking-water quality.". *WHO Chronicle*, **38**:104–108, 2011.

[3] T. F. Clasen and A. Bastable. "Faecal contamination of drinking water during collection and household storage: the need to extend protection to the point of use. ". *Journal of Water and Health*, **1**:109–115, 2003.

[4] N. Aboualigaledari and M. Rahmani. "A review on the synthesis of the TiO_2-based photocatalyst for the environmental purification.". *Journal of Composites and Compounds*, **3**:25–42, 2021.

[5] E. Jones, M. Qadir, M. T. van Vliet, V. Smakhtin, and S-M. Kang. "The state of desalination and brine production: A global outlook. ". *Science of the Total Environment*, **657**:1343–1356, 2019.

[6] G. Doornbusch, M. van der Wal, M. Tedesco, J. Post, K. Nijmeijer, and Z. Borneman. "Multistage electrodialysis for desalination of natural seawater.". *Desalination*, **505**:114973, 2021.

[7] M. Kerwick, S. Reddy, A. Chamberlain, and D. Holt. "Electrochemical disinfection, an environmentally acceptable method of drinking water disinfection?". *Electrochimica Acta*, **50**:5270–5277, 2005.

[8] A. J. Rad. "Synthesis of copper oxide nanoparticles on activated carbon for pollutant removal in Tartrazine structure.". *Journal of Composites and Compounds*, **2**:99–104, 2020.

[9] C. Liu, X. Xie, W. Zhao, N. Liu, P. A. Maraccini, L. M. Sassoubre, A. B. Boehm, and Y. Cui. "Conducting nanosponge electroporation for affordable and high-efficiency disinfection of bacteria and viruses in water.". *Nano letters*, **13**:4288–4293, 2013.

[10] S. Hussain, N. de Las Heras, H. Asghara, N. Brown, and E. Roberts. "Disinfection of water by adsorption combined with electrochemical treatment.". *Water Research*, **54**:170–178, 2014.

[11] L. Guo, K. Ding, K. Rockne, M. Duran, and B. P. Chaplin. "Bacteria inactivation at a sub-stoichiometric titanium dioxide reactive electrochemical membrane.". *Journal of Hazardous Materials*, **319**:137–146, 2016.

[12] J. Jeong, J. Y. Kim, M. Cho, W. Choi, and J. Yoon. "Inactivation of Escherichia coli in the electrochemical disinfection process using a Pt anode.". *Chemosphere*, **67**:652–659, 2007.

[13] X. Tan, C. Chen, Y. Hu, J. Wen, Y. Qin, J. Cheng, and Y. Chen. "Novel AgNWs-PAN/TPU membrane for point-of-use drinking water electrochemical disinfection.". *Science of the Total Environment*, **637**:408–417, 2018.

[14] S. Eskandarinezhad, R. Khosravi, M. Amarzadeh, P. Mondal, and F. J. C. Magalhães Filho. "Application of different Nanocatalysts in industrial effluent treatment: A review.". *Journal of Composites and Compounds*, **3**:43–56, 2021.

[15] M. Arefian, M. Hojjati, I. Tajzad, A. Mokhtarzade, M. Mazhar, and A. Jamavari. "A review of Polyvinyl alcohol/Carboxymethyl cellulose (PVA/CMC) composites for various applications.". *Journal of Composites and Compounds*, **2**:69–76, 2020.

[16] A. Moghanian, A. Ghorbanoghli, M. Kazem-Rostami, A. Pazhouheshgar, E. Salari, M. Saghafi Yazdi, T. Alimardani, H. Jahani, F. Sharifian Jazi, and M. Tahriri. "Novel antibacterial Cu/Mg-substituted 58S-bioglass: Synthesis, characterization and investigation of in vitro bioactivity.". *International Journal of Applied Glass Science*, **11**:685–698, 2020.

[17] A. Greiner and J. H. Wendorff. "Electrospinning: a fascinating method for the preparation of ultrathin fibers.". *Angewandte Chemie International Edition*, **46**:5670–5703, 2007.

[18] C. Gao, W. Deng, F. Pan, X. Feng, and Y. Li. "Superhydrophobic electrospun PVDF membranes with silanization and fluorosilanization co-functionalized CNTs for improved direct contact membrane distillation.". *Engineered Science*, **9**:35–43, 2020.

[19] S. Abedini, N. Parvin, P. Ashtari, and F. Jazi. "Microstructure, strength and CO_2 separation characteristics of α-alumina supported γ-alumina thin film membrane.". *Advances in Applied Ceramics*, **112**:17–22, 2013.

[20] L. Bazli, M. Siavashi, and A. Shiravi. "A review of carbon nanotube/TiO_2 composite prepared via sol-gel method. ". *Journal of Composites and Compounds*, **1**: 1–9, 2019.

[21] M. Radmansouri, E. Bahmani, E. Sarikhani, K. Rahmani, F. Sharifianjazi, and M. Irani. "Doxorubicin hydrochloride-Loaded electrospun chitosan/cobalt ferrite/titanium oxide nanofibers for hyperthermic tumor cell treatment and controlled drug release.". *International Journal of Biological Macromolecules*, **116**: 378–384, 2018.

[22] F. Safeeda Nv, J. Gopinathan, B. Indumathi, S. Thomas, and A. Bhattacharyya. "Morphology and hydroscopic properties of acrylic/thermoplastic polyurethane core–shell electrospun micro/nano fibrous mats with tunable porosity.". *RSC Advances*, **6**: 54286–54292, 2016.

[23] M. A. Jahid, J. Hu, and S. Thakur. "Novel approach of making porous polyurethane membrane and its properties for apparel application.". *Journal of Applied Polymer Science*, **137**:48566, 2020.

[24] D. K. Chattopadhyay and D. C. Webster. "Thermal stability and flame retardancy of polyurethanes.". *Progress in Polymer Science*, **34**:1068–1133, 2009.

[25] P. Panda and B. Sahoo. "Synthesis and applications of electrospun nanofibers-a review.". *Nanotechnology*, **1**:399–416, 1990.

[26] R. J. Zdrahala and I. J. Zdrahala. "Biomedical applications of polyurethanes: a review of past promises, present realities, and a vibrant future.". *Journal of Biomaterials Applications*, **14**:67–90, 1999.

[27] H. Zhuo, J. Hu, and S. Chen. "Coaxial electrospun polyurethane core-shell nanofibers for shape memory and antibacterial nanomaterials.". *Express Polymer Letters*, **5**:182–187, 2011.

[28] T. A. Adegbola, O. Agboola, and O. S. I. Fayomi. "Review of polyacrylonitrile blends and application in manufacturing technology: recycling and environmental impact.". *Results in Engineering*, **7**:100144, 2020.

[29] M. Kutz. *" Applied plastics engineering handbook: processing, materials, and applications."*, volume . William Andrew, 2016.

[30] M. Iqbal, D. K. Dinh, Q. Abbas, M. Imran, H. Sattar, and A. Ul Ahmad. "Controlled surface wettability by plasma polymer surface modification.". *Surfaces*, **2**: 349–371, 2019.

[31] M. Kehrer, J. Duchoslav, A. Hinterreiter, A. Mehic, T. Stehrer, and D. Stifter. "Surface functionalization of polypropylene using a cold atmospheric pressure plasma jet with gas water mixtures.". *Surface and Coatings Technology*, **384**:125170, 2020.

[32] M. Sanchis, V. Blanes, M. Blanes, D. Garcia, and R. Balart. "Surface modification of low density polyethylene (LDPE) film by low pressure O_2 plasma treatment.". *European Polymer Journal*, **42**:1558–1568, 2006.

[33] A. Savolainen, J. Kuusipalo, and H. Karhuketo. "Extrusion coating. I, Corona after-treatment of LDPE coating.". *Tappi Journal*, **73**:133–139, 1990.

[34] I. Novák and Š. Florián. "Influence of ageing on adhesive properties of polypropylene modified by discharge plasma.". *Polymer International*, **50**:49–52, 2001.

[35] J. M. Strobel, M. Strobel, C. S. Lyons, C. Dunatov, and S. J. Perron. "Aging of air-corona-treated polypropylene film.". *Journal of Adhesion Science and Technology*, **5**:119–130, 1991.

[36] S. Guimond and M. R. Wertheimer. "Surface degradation and hydrophobic recovery of polyolefins treated by air corona and nitrogen atmospheric pressure glow discharge).". *Journal of Applied Polymer Science*, **94**: 1291–1303, 2004.

[37] J. M. Farley and P. Meka. "Heat sealing of semicrystalline polymer films. III. Effect of corona discharge treatment of LLDPE.". *Journal of Applied Polymer Science*, **51**:121–131, 1994.

[38] J. Lahti. "Dry toner-based electrophotographic printing on extrusion coated paperboard.". , 2005.

[39] M. Ataeefard. "Study of PLA printability with flexography ink: Comparison with common packaging polymer.". *Progress in Color, Colorants and Coatings*, **12**:101–105, 2019.

[40] R. Bollström, M. Tuominen, A. Määttänen, J. Peltonen, and M. Toivakka. "Top layer coatability on barrier coatings.". *Progress in Organic Coatings*, **73**: 26–32, 2012.

[41] T. Schuman, M. Wikström, and M. Rigdahl. "Coating of surface-modified papers with poly (vinyl alcohol).". *Surface and Coatings Technology*, **183**:96–105, 2004.

[42] J. Junnila, A. Savolainen, and D. Forsberg. "Adhesion improvements between paper and polyethylene by pretreatment of substrate, polymers.". *Laminations and Coatings Conference, Orlando, FL, USA.*, :5–8, 1989.

[43] A. Popelka, P. N. Khanam, and M. A. AlMaadeed. "Surface modification of polyethylene/graphene composite using corona discharge.". *Journal of Physics D: Applied Physics*, **51**:105302, 2018.

[44] H. R. Ghorbani and M. Molaei. "Antibacterial nanocomposite preparation of polypropylene-Silver using Corona discharge.". *Progress in Organic Coatings*, **112**:187–190, 2017.

[45] A. Popelka, I. Novák, M. A. S. Al-Maadeed, M. Ouederni, and I. Krupa. "Effect of corona treatment on adhesion enhancement of LLDPE.". **335**:118–125, 2018.

[46] V. C. Louzi and J. S. de Carvalho Campos. "Corona treatment applied to synthetic polymeric monofilaments (PP, PET, and PA-6).". *Surfaces and Interfaces*, **14**:98–107, 2019.

[47] M. Y. Alekseeva, V. Dryakhlov, M. Galikhanov, I. Nizameev, and I. Shaikhiev. "Enhancement of separation of water–oil emulsion using unipolar corona-treated polysulfonamide membranes.". *Petroleum Chemistry*, **58**:152–156, 2018.

[48] J. Pinson and D. Thiry. *"Surface modification of polymers, methods and applications. "*, volume . Wiley, 2019.

[49] J. Gopinathan, B. Indumathi, S. Thomas, and A. Bhattacharyya. "Morphology and hydroscopic properties of acrylic/thermoplastic polyurethane core–shell electrospun micro/nano fibrous mats with tunable porosity.". *RSC Advances*, **6**:54286–54292, 2016.

[50] J. Bharath, M. Mosodeen, S. Motilal, S. Sandy, S. Sharma, T. Tessaro, K. Thomas, M. Umamaheswaran, D. Simeon, and A. Adesiyun. "Microbial quality of domestic and imported brands of bottled water in Trinidad". *International Journal of Food Microbiology*, **81**:53–62, 2003.

[51] K. M. Wright, P. J. Wright, and N. J. Holden. "MacConkey broth purple provides an efficient MPN estimation method for Shigatoxigenic *Escherichia coli*.". *Journal of Microbiological Methods*, **181**:106132, 2021.

[52] H. S. Mahmood and M. K. Jawad. "Antibacterial activity of chitosan/PAN blend prepared at different ratios, AIP Conference Proceedings.". *AIP Publishing LLC.*, **32**:020078, 2019.

[53] J. Li, S. Su, L. Zhou, V. Kundrát, A. M. Abbot, F. Mushtaq, D. Ouyang, D. James, D. Roberts, and H. Ye. "Carbon nanowalls grown by microwave plasma enhanced chemical vapor deposition during the carbonization of polyacrylonitrile fibers.". *Journal of Applied Physics*, **113**:024313, 2013.

[54] E. Zdraveva, B. Mijovic, E. Govorcin Bajsic, and V. Grozdanic. "The efficacy of electrospun polyurethane fibers with TiO_2 in a real time weathering condition.". *Textile Research Journal*, **88**:2445–2453, 2018.

[55] L. Tong, X-X. Wang, X-X. He, G-D. Nie, J. Zhang, B. Zhang, W-Z. Guo, and Y. Z. Long. "Electrically conductive TPU nanofibrous composite with high stretchability for flexible strain sensor.". *Nanoscale Research Letters*, **13**:1–8, 2018.

[56] A. B. D. Nandiyanto, R. Oktiani, and R. Ragadhita. "How to read and interpret FTIR spectroscope of organic material.". *Indonesian Journal of Science and Technology*, **4**:97–118, 2019.

[57] Y. Ren, T. Huo, Y. Qin, and X. Liu. "Preparation of flame retardant polyacrylonitrile fabric based on sol-gel and layer-by-layer assembly.". *Materials*, **11**:483, 2018. DOI: https://doi.org/10.3390/ma11040483.

[58] L. Tong, X. X. Wang, X. X. He, et al. " Electrically conductive TPU nanofibrous composite with high stretchability for flexible strain sensor.". *Nanoscale Research Letters*, **13**:86, 2018. DOI: https://doi.org/10.1186/s11671-018-2499-0.

[59] A. M. Assiry, M. H. Gaily, M. Alsamee, and A. Sarifudin. "Electrical conductivity of seawater during ohmic heating.". *Desalination*, **260**:9–17, 2010.

[60] F. E. Ahmed, B. S. Lalia, and R. Hashaikeh. "A review on electrospinning for membrane fabrication: Challenges and applications.". *Desalination*, **356**:15–30, 2015.

[61] S. Hu, K. Wu, H. Wang, and J. Chen. "Electrical conductivity measurement method in seawater desalination based on variable frequency excitation.". *9th International Conference on Electronic Measurement & Instruments, IEEE*, :810–813, 2009.

[62] J. Cai, X. Liu, Y. Zhao, and F. J. D. Guo. "Membrane desalination using surface fluorination treated electrospun polyacrylonitrile membranes with nonwoven structure and quasi-parallel fibrous structure.". *Desalination*, **429**:70–75, 2018.

[63] Y. Li, E. Wong, Z. Mai, and B. Van der Bruggen. "Fabrication of composite polyamide/Kevlar aramid nanofiber nanofiltration membranes with high permselectivity in water desalination.". *Journal of Membrane Science*, **592**:117396, 2019.

[64] S. Kaur, R. Barhate, S. Sundarrajan, T. Matsuura, and S. Ramakrishna. "Hot pressing of electrospun membrane composite and its influence on separation performance on thin film composite nanofiltration membrane.". *Desalination*, **279**:201–109, 2011.

[65] L. D. Tijing, Y. C. Woo, M. A. H. Johir, J. S. Choi, and H. K. Shon. "A novel dual-layer bicomponent electrospun nanofibrous membrane for desalination by direct contact membrane distillation.". *Chemical Engineering Journal*, **256**:155–159, 2014.

[66] M. Talaeipour, J. Nouri, A. H. Hassani, and A. H. Mahvi. "An investigation of desalination by nanofiltration, reverse osmosis and integrated (hybrid NF/RO) membranes employed in brackish water treatment.". *Journal of Environmental Health Science and Engineering*, **15**:18, 2017.